# Electronic Supplementary Information

**Experimental Section**

**Materials:** Radix cynanchi paniculati was obtained from the local KouDai Pharmacy (Haozhou, China). Sodium hydroxide (NaOH), ammonium chloride (NH$_4$Cl), salicylic acid (C$_7$H$_6$O$_3$), sodium citrate dehydrate (C$_6$H$_5$Na$_3$O$_7$·2H$_2$O), *p*-dimethylaminobenzaldehyde (C$_9$H$_{11}$NO), Nafion solution (5 wt%), sodium nitroferricyanide dihydrate (C$_5$FeN$_6$Na$_2$O·2H$_2$O), sodium nitrite (NaNO$_2$), cobalt nitrate (Co(NO$_3$)$_2$) and sodium hypochlorite (NaClO) were purchased from Aladdin Ltd. (Shanghai, China). Sulfuric acid (H$_2$SO$_4$), hydrogen peroxide (H$_2$O$_2$), hydrazine monohydrate (N$_2$H$_4$·H$_2$O) and ethyl alcohol (C$_2$H$_5$OH) were purchased from Beijing Chemical Corp. (China). chemical Ltd. in Chengdu. All reagents used in this work were analytical grade without further purification.

**Synthesis of Co@RCPC：** The Radix Cynanchi Paniculati was washed with ethanol and deionized water, and then dried at 60 °C. After that, 0.15 g of pretreated radix cynanchi paniculati was directly immersed into the 40 mL 0.1 M Co(NO$_3$)$_2$·H$_2$O solution for overnight and dried at 60 °C under vacuum. Subsequently, this sample was annealed at 800 °C in Ar atmosphere for 2 h with a heating speed of 2 °C min$^{-1}$. Lastly, the Co@RCPC was collected after cooled to ambient temperature. In addition, the control sample RCPC was obtained via annealing Radix Cynanchi Paniculati without the presence of Co salt under otherwise identical conditions.

**Preparation of Co@RCPC/CC and RCPC/CC：** Typically, 5 mg of catalyst and 20 μL of 5 wt% Nafion solution were dispersed in 480 μL of water/ethanol solution (v/v = 1:3) by sonicating for 1 h to form a uniform ink. Then 20 μL of the above dispersion was loaded onto a CC (0.25 cm$^2$) and dried under ambient conditions.

**Preparation of Co/CC:** Briefly, The Co nanoparticles were prepared by pyrolysis of 0.291 g of Co(NO$_3$)$_2$·6H$_2$O at 500 °C for 2 h in H$_2$/Ar atmosphere. The Co powder was prepared into ink and dropped on CC, then dried in air, Co/CC was finally obtained.

**Characterizations:** XRD data were acquired by a LabX XRD-6100 X-ray

diffractometer with a Cu Kα radiation (40 kV, 30 mA) of wavelength 0.154 nm (SHIMADZU, Japan). SEM measurements were carried out on a Gemini SEM 300 scanning electron microscope (ZEISS, Germany) at an accelerating voltage of 5 kV. XPS measurements were performed on an ESCALABMK II X-ray photoelectron spectrometer using Mg as the exciting source. The absorbance data of spectrophotometer was measured on UV-Vis spectrophotometer. TEM image was obtained from a Zeiss Libra 200FE transmission electron microscope operated at 200 kV. r. Gas chromatography (GC-2014C, SHIMADZU) was used to quantitatively detect $H_2$ and $N_2$.

**Electrochemical measurements:** All electrochemical measurements were carried on the CHI 760E electrochemical workstation (Shanghai, Chenhua) using a standard three-electrode setup. Electrolyte solution was Ar-saturated of 0.1 M NaOH with 0.1 M $NO_2^-$, using Co@RCPC/CC (0.5 cm × 0.5 cm) as the working electrode, graphite rod as the counter electrode and a Hg/HgO as the reference electrode. We use a H-type electrolytic cell separated by a Nafion 117 membrane which was protonated by boiling in $H_2O_2$ (5%) aqueous solution and 0.5 M $H_2SO_4$ at 80 °C for 2 h, respectively, and then boiling in ultrapure water for another 2 h. All the potentials reported in our work were converted to reversible hydrogen electrode via calibration with the following equation: E (RHE) = E (Hg/HgO) + (0.098 + 0.0591 × pH) V and the presented current density was normalized to the geometric surface area. Linear sweep voltammetry (LSV) tests were performed at the rate of 5 mV $s^{-1}$ from 0.2 to −1.0 V. To have a good sealing, the H-shaped cell is decorated with kinds of lid. The speed of gas input and output is nearly the same. The whole experiment was performed under ambient conditions.

**Determination of $NH_3$:** $NH_3$ concentration in the solution was determined by colorimetry (the obtained electrolyte was diluted 50 times) using the indophenol blue method.[1] In detail, 2 mL of the solution after reaction, and 2 mL of 1 M NaOH coloring solution containing 5% salicylic acid and 5% sodium citrate. Then, 1 mL oxidizing solution of 0.05 M NaClO and 0.2 mL catalyst solution of $C_5FeN_6Na_2O$ (1

wt%) were added to the above solution. After standing in the dark for 2 h, the UV-Vis absorption spectra were measured. The concentration of $NH_3$ was identified using the absorbance at a wavelength of 655 nm. The concentration-absorbance curve was calibrated using the standard $NH_4Cl$ solution with $NH_3$ concentrations of 0, 0.2, 0.5, 1.0, 2.0 and 5.0 ppm in 0.1 M NaOH solution. The fitting curve (y = 0.3795x + 0.0347, $R^2$ = 0.9997) shows good linear relation of absorbance value with $NH_3$ concentration.

**Determination of $N_2H_4$:** In this work, we used the method of Watt and Chrisp to estimate whether $N_2H_4$ produced.[2] The chromogenic reagent was a mixed solution of 5.99 g $C_9H_{11}NO$, 30 mL HCl and 300 mL $C_2H_5OH$. In detail, 1 mL electrolyte was added into 1 mL prepared color reagent and standing for 15 min in the dark. The absorbance at 455 nm was measured to quantify the $N_2H_4$ concentration with a standard curve of hydrazine (y = 0.6788x + 0.0879, $R^2$ = 0.9994).

**Determination of $N_2$ and $H_2$:** $N_2$ and $H_2$ were quantified by GC.

**Calculations of the FE and $NH_3$ yield rate:**

The amount of $NH_3$ ($m_{NH3}$) was calculated by the following equation:

$$m_{NH3} = [NH_3] \times V$$

$NH_3$ FE was calculated by the following equation:

$$FE = (6 \times F \times [NH_3] \times V) / (M_{NH3} \times Q) \times 100\%$$

$NH_3$ yield was calculated using the following equation:

$$NH_3 \text{ yield} = ([NH_3] \times V) / (M_{NH3} \times t \times A)$$

Where F is the Faradic constant (96485 C $mol^{-1}$), $[NH_3]$ is the $NH_3$ concentration, V is the volume of electrolyte in the anode compartment (60 mL), $M_{NH3}$ is the molar mass of $NH_3$ molecule, Q is the total quantity of applied electricity; t is the electrolysis time (1 h) and A is the geometric area of the working electrode (0.5 × 0.5 $cm^{-2}$).

The calculation of partial current densities involves multiplying the average current density at each potential by the FE of each reduction product.
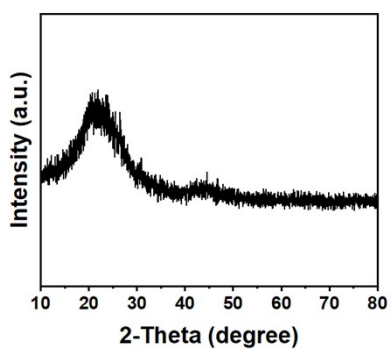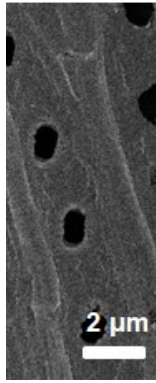
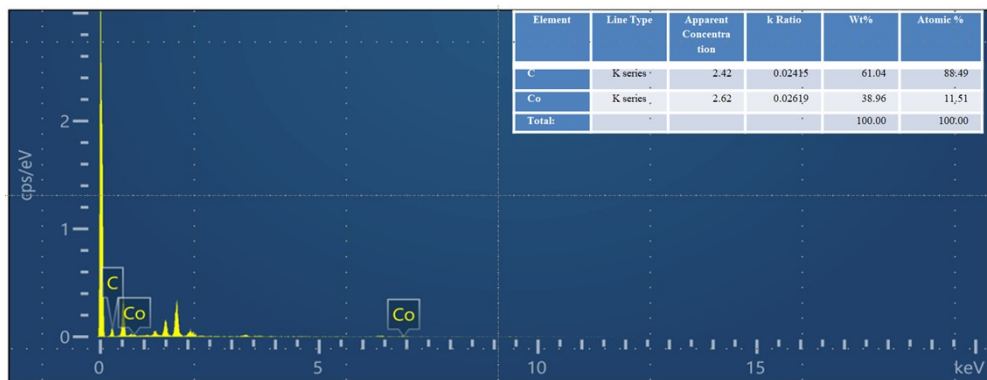**Fig. S1.** XRD pattern of RCPC.

**Fig. S2.** SEM image of RCPC.

| Element | Line Type | Apparent Concentration | k Ratio | Wt% | Atomic % |
|---------|-----------|------------------------|---------|-------|----------|
| C | K series | 2.42 | 0.02415 | 61.04 | 88.49 |
| Co | K series | 2.62 | 0.02619 | 38.96 | 11,51 |
| Total: | | | | 100.00 | 100.00 |

**Fig. S3.** EDX spectrum of Co@RCPC.
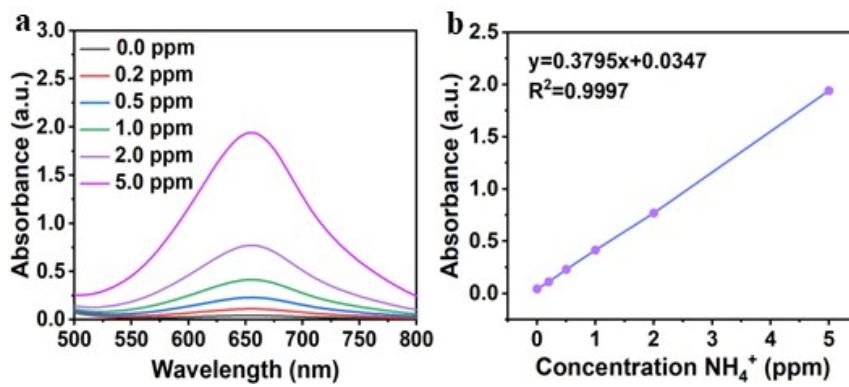
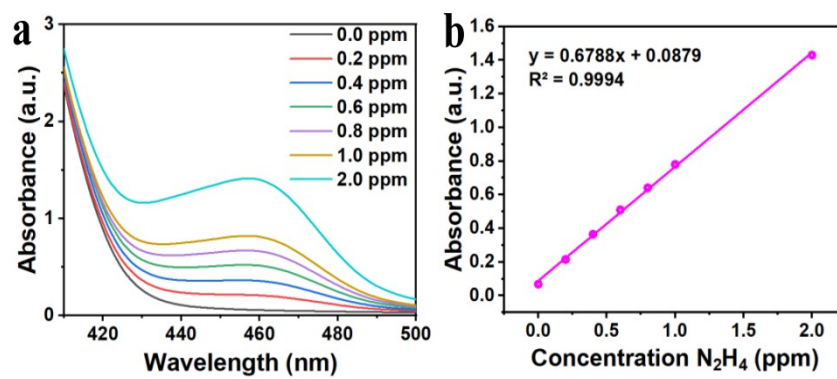**Fig. S4.** (a) UV-vis absorption spectra and (b) corresponding calibration curve for calculation of $NH_4^+$ concentration.

**Fig. S5.** (a) UV-Vis absorption spectra and corresponding (b) calibration curve used for calculation of $N_2H_4$ concentration.
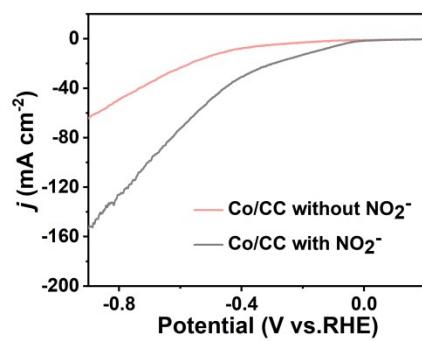
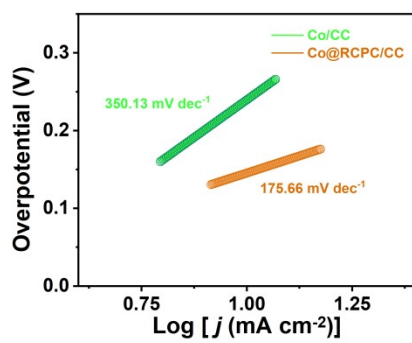**Fig. S6.** LSV curves of Co/CC in 0.1 M NaOH with/without 0.1 M $NO_2^-$.

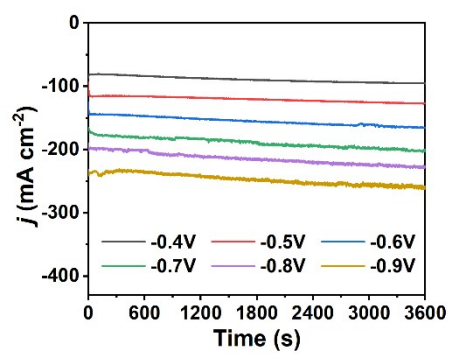**Fig. S7.** Tafel plots for Co@RCPC/CC and Co/CC in 0.1 M NaOH with 0.1 M $NO_2^-$.

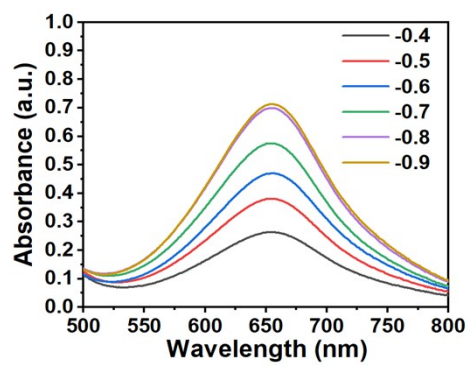**Fig. S8.** CA curves of Co@RCPC/CC for $NO_2^-RR$ at different potentials.

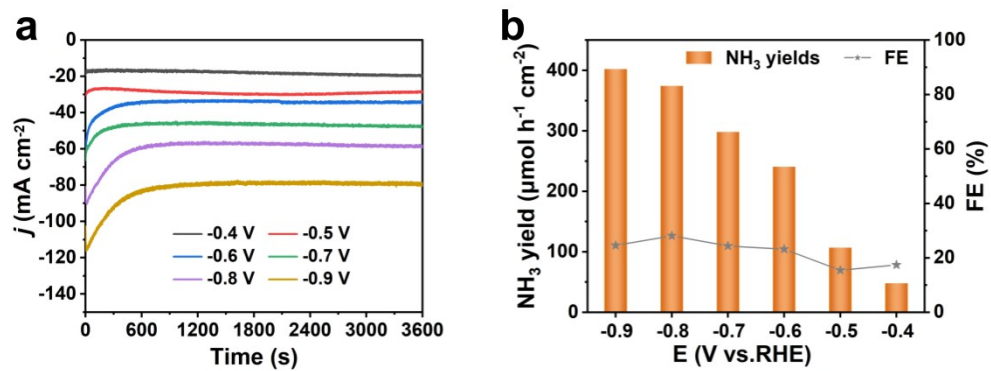**Fig. S9.** UV-vis spectra of NH$_3$ at different given potentials.

**Fig. S10.** (a) CA curves of RCPC/CC for $NO_2^-RR$ at different potentials. (b) $NH_3$ yields and FEs of RCPC/CC at different given potentials.
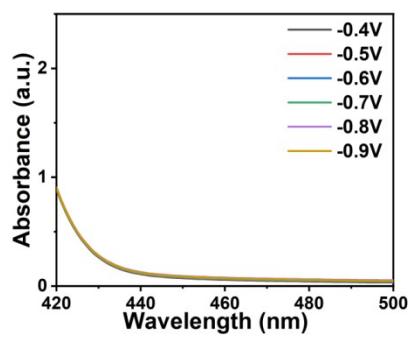
**Fig. S11.** UV-vis spectra of $N_2H_4$ at different given potentials.
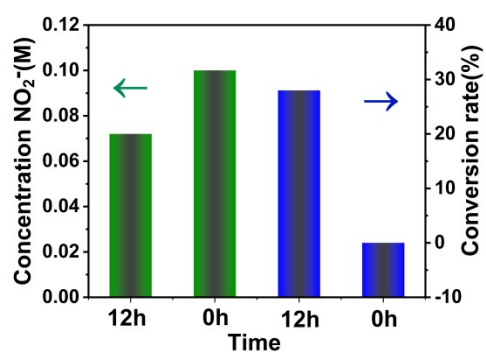
**Fig. S12.** Conversion rates and concentrations of $NO_2^-$ during 12 h electrolysis at $-0.8$ V.
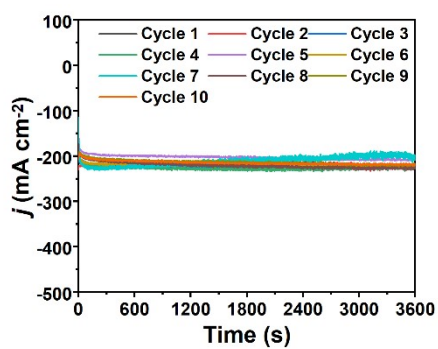
**Fig. S13.** CA curves of Co@RCPC/CC during recycling tests toward $NO_2^-$RR at −0.8 V.
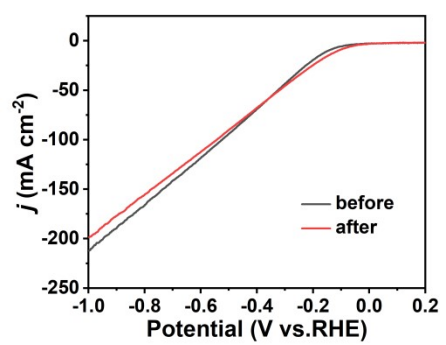
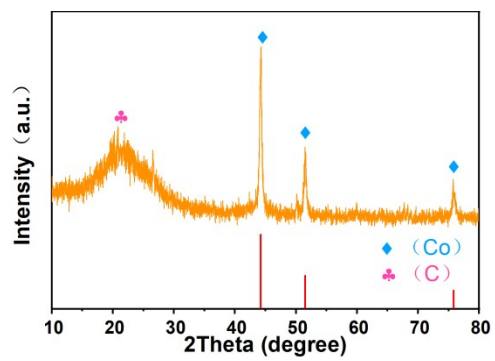**Fig. S14.** LSV curves of Co@RCPC/CC before and after long-term stability test.

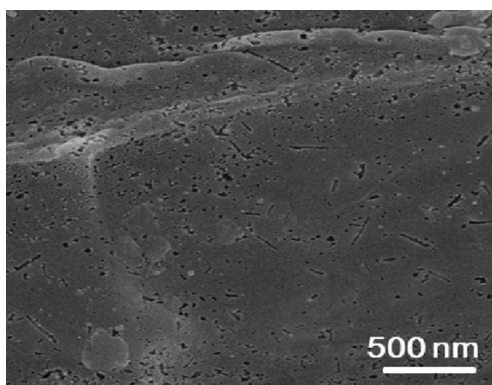**Fig. S15.** XRD of Co@RCPC/CC after long-term stability test.

**Fig. S16.** SEM of Co@RCPC/CC after long-term stability test.

**Table S1** Comparison of the catalytic performance of Co@RCPC/CC with other reported $NO_2^-$RR electrocatalysts under ambient conditions.

| Catalyst | Electrolyte | Potential (V vs. RHE) | NH₃ yield ($\mu mol\ h^{-1}\ cm^{-2}$) | FE (%) | Ref. |
|---|---|---|---|---|---|
| **Co@RCPC/CC** | **0.1 M NaOH (0.1 M NaNO₂)** | **−0.8** | **1261.66** | **92.77** | **This work** |
| CoP/CC | 1.0 M NaOH (2mM NaNO₂) | −0.3 | 22.35 | 91.6 | 3 |
| Ni-NSA-$V_{Ni}$ | 0.2 M Na₂SO₄ (200 ppm NaNO₂) | −0.54 | 235.5□ | 88.9 | 4 |
| Fe₂P/AS/CP | 0.1 M KOH (100 mM NO₂⁻) | −0.5 | 1594.5 | 96.8 | 5 |
| NiS₂@TiO₂/TM | 0.1 M NaOH (0.1 M NaNO₂) | −0.5 | 591.9 | 92.1 | 6 |
| Cu@Cu₂O NPs | 1.0 M Na₂SO₄ (100 ppm NaNO₂) | – | 30 | 94 | 7 |
| CoP NA/TM | 0.1 M PBS (500 ppm NaNO₂) | −0.2 | 132.7 | 90.0 | 8 |
| MnO₂ nanoarrays | 0.1 M Na₂SO₄ (5 mM NaNO₂) | −1.75 | $8.6 \times 10^{-12}$ | 6.0 | 9 |
| Ni@MDC/CP | 0.1 M NaOH (0.1 M NaNO₂) | −0.8 | 370.6□ | 65.4 | 10 |
| CoB nanoarray | 0.1 M Na₂SO₄ (400 ppm NaNO₂) | −0.5 | 233.1 | 95.2 | 11 |
| CuNi alloys | 0.1 M NaOH (0.01 M NaNO₂) | −1.2 | – | 96 | 12 |
| FeP@TiO₂/TP | 0.1 M NaOH (0.1 M NaNO₂) | −0.5 | 346.6 | 97.1 | 13 |
| Ni@JBC-800 | 0.1 M NaOH (0.1 M NaNO₂) | −0.5 | 242.2 | 83.4 | 14 |
| Cu/JDC/CP | 0.1 M NaOH (0.1 M NaNO₂) | −0.6 | 523.5 | 93.2 | 15 |
| C-NiWO₄/NF | 0.1 M NaOH (0.1 M NaNO₂) | −0.4 | 645.6 | 97.6 | 16 |
| Pd/CuO NOs | 0.1 M K₂SO₄ (0.01M KNO₂) | −1.5 ( V vs. SCE) | 906.4 ($\mu g\ h^{-1}\ mg^{-1}_{cat}$) | 91.8 | 17 |
| Ru SA-NC | 0.5M NO2⁻ (1.0 M KOH) | −0.6 | – | 97.8 | 18 |

# References

1   D. Zhu, L. Zhang, R. E. Ruther and R. J. Hamers, *Nat. Mater.*, 2013, **12**, 836–841.

2   L. C. Green, D. A. Wagner, J. Glogowski, P. L. Skipper, J. S. Wishnok and S. R. Tannenbaum, *Anal. Biochem.*, 1982, **126**, 131–138.

3   H. Zhang, G. Wang, C. Wang, Y. Liu, Y. Yang, C. Wang, W. Jiang, L. Fu and J. Xu, *J. Electroanal. Chem.*, 2022, **910**, 116171.

4   C. Wang, W. Zhou, Z. Sun, Y. Wang, B. Zhang and Y. Yu, *J. Mater. Chem. A*, 2021, **9**, 239–243.

5   J. Hu, T. Zhao, H. Zhang, X. Li, A. Shi, X. Li, Q. Wang and G. Hu, *Surf. Interfaces*, 2023, **38**, 102818.

6   X. He, L. Hu, L. Xie, Z. Li, J. Chen, X. Li, J. Li, L. Zhang, X. Fang, D. Zheng, S. Sun, J. Zhang, A. Ali Alshehri, Y. Luo, Q. Liu, Y. Wang and X. Sun, *J. Colloid Interface Sci.*, 2023, **634**, 86–92.

7   S. Yeon, S. J. Lee, J. Kim, T. Begildayeva, A. Min, J. Theerthagiri, M. L. A. Kumari, L. M. C. Pinto, H. Kong and M. Y. Choi, *Environ. Res.*, 2022, **215**, 114154.

8   G. Wen, J. Liang, Q. Liu, T. Li, X. An, F. Zhang, A. A. Alshehri, K. A. Alzahrani, Y. Luo, Q. Kong and X. Sun, *Nano Res.*, 2022, **15**, 972–977.

9   R. Wang, Z. Wang, X. Xiang, R. Zhang, X. Shi and X. Sun, *Chem. Commun.*, 2018, **54**, 10340–10342.

10  X. He, X. Li, X. Fan, J. Li, D. Zhao, L. Zhang, S. Sun, Y. Luo, D. Zheng, L. Xie, A. M. Asiri, Q. Liu and X. Sun, *ACS Appl. Nano Mat.*, 2022, **5**, 14246–14250.

11  L. Hu, D. Zhao, C. Liu, Y. Liang, D. Zheng, S. Sun, Q. Li, Q. Liu, Y. Luo, Y. Liao, L. Xie and X. Sun, *Inorg. Chem. Front.*, 2022, **9**, 6075–6079.

12  L. Mattarozzi, S. Cattarin, N. Comisso, P. Guerriero, M. Musiani, L. Vázquez-Gómez and E. Verlato, *Electrochim. Acta*, 2013, **89**, 488–496.

13   A. Zhang, Y. Liang, X. He, X. Fan, C. Yang, L. Ouyang, D. Zheng, S. Sun, Z. Cai, Y. Luo, Q. Liu, S. Alfaifi, L. Cai, H. Wang and X. Sun, *Inorg. Chem.*, 2023, **62**, 12644–12649.

14   X. Li, Z. Li, L. Zhang, D. Zhao, J. Li, S. Sun, L. Xie, Q. Liu, A. A. Alshehri, Y. Luo, Y. Liao, Q. Kong and X. Sun, *Nanoscale*, 2022, **14**, 13073–13077.

15   L. Ouyang, L. Yue, Q. Liu, Q. Liu, Z. Li, S. Sun, Y. Luo, A. Ali Alshehri, M. S. Hamdy, Q. Kong and X. Sun, *J. Colloid Interface Sci.*, 2022, **624**, 394–399.

16   H. Qiu, Q. Chen, J. Zhang, X. An, Q. Liu, L. Xie, W. Yao, X. Sun and Q. Kong, *Inorg. Chem. Front.*, 2023, **10**, 3909–3915.

17   S. Liu, L. Cui, S. Yin, H. Ren, Z. Wang, Y. Xu, X. Li, L. Wang and H. Wang, *Appl. Catal. B Environ.*, 2022, **319**, 121876.

18   Z. Ke, D. He, X. Yan, W. Hu, N. Williams, H. Kang, X. Pan, J. Huang, J. Gu and X. Xiao, *ACS Nano*, 2023, **17**, 3483-3491.